DYNAMICS OF NON-PREMIXED V-GUTTER STABILIZED FLAMES IN HIGH TEMPERATURE FLOW

A Thesis
Presented to
The Academic Faculty

by

Aimee N. Fricker

In Partial Fulfillment
of the Requirements for the Degree
Bachelor of Science in the
School of Aerospace Engineering

Georgia Institute of Technology
May 2010

DYNAMICS OF NON-PREMIXED V-GUTTER STABILIZED FLAMES IN HIGH TEMPERATURE FLOW

Approved by:

Dr. Ben Zinn, Advisor
School of Aerospace Engineering
Georgia Institute of Technology

Dr. Eugene Lubarsky
School of Aerospace Engineering
Georgia Institute of Technology

Date Approved: 05/07/2010

TABLE OF CONTENTS

	Page
LIST OF FIGURES	iv
LIST OF SYMBOLS AND ABBREVIATIONS	v
SUMMARY	vi
CHAPTER	
1 Introduction	1
2 Experimental Methodology	8
Description of Test Facility and Instrumentation	8
Using High Speed Photography to Quantify Oscillatory Heat Release	9
Quantification of Stationary Heat Release Using 3-Camera Spectroscopy	12
3 Results and Discussion	14
Oscillatory Heat Release	15
Measurements of Flame Oscillations due to BVK Asymmetric Vorticity	15
Von-Kármán Asymmetric Vortex Shedding	18
Stationary Heat Release	21
4 Conclusions	25
REFERENCES	27

LIST OF FIGURES

Page

Figure 1. Fluid Mechanics of Isothermal Bluff Body Flow[1] 3

Figure 2. Photograph of SFC Test Facility 8

Figure 3. Schematic of Single Flameholder Combustor (SFC) Test Facility identifying major components of the rig and V-gutter flame holder 9

Figure 4. Methodology for recording flame dynamics at a given cross section 10

Figure 5. 2D Digital Fourier Transform (DFT) of the time history data set and method for generating spectra of flame oscillations, showing: 11

Figure 6. Schematic of three-camera technique used for mean heat release characterization 12

Figure 7. Measured Jet-A flame spectra and light bands used for image processing 13

Figure 8. Summary of experimental operating conditions expressed as Φ_{global} vs. DeZubay's Correlation 15

Figure 9. Sequence of flame images representing one period of BVK Oscillations. Flow conditions: V_{in}=230 m/s, T=860ºC, Φ_{global}~0.95 16

Figure 10. (a) Time history, (b) 2D DFT, and (c) spectra of flame at M=0.340, Φ =0.991, 859°C, 14.43% O2, W=1.750in 17

Figure 11. Variation of Q' along the axial length of the combustor. 18

Figure 12. Dependence of Von-Kármán oscillation intensity on equivalence ratio 19

Figure 13. Intensity of von-Kármán oscillations versus fuel-jet penetration 21

Figure 14. Stationary Heat Release Images for M=0.390, T838°C, W=2.000" 22

Figure 15. Average CH* Profile for Constant DeZubay Parameter 23

Figure 16. Shear layer definition (M=0.348, T=764C, Phiglobal=0.512) 24

Figure 17. BVK Oscillation Intensity versus the ratio of heat release in the shear layer 24

LIST OF SYMBOLS AND ABBREVIATIONS

V	Velocity
M	Mach Number
T	Temperature
T_b	Temperature of burned products
T_u	Temperature of un-burned reactants
Z	DeZubay's Parameter
Z(T)	DeZubay's Parameter with temperature correction
q	Fuel-Air momentum flux ratio
P	Pressure
D	Flame holder width
W	V-gutter Width
q′	Oscillatory heat release
d	Fuel injector diameter
x	Fuel penetration distance
z	Distance from fuel injector
SFC	Single flame-holder combustor
2D DFT	Two-dimensional discrete Fourier Transform
$\%O_2$	Oxygen Percentage of incoming air

SUMMARY

This study investigated the dynamics of bluff body stabilized combustion of liquid fuel jets injected into the cross flow of preheated air just upstream of V-guttered bluff body's wake. The dynamics of investigated combustion process were determined by using advanced analytical methods to analyze high speed movies of the combustion process and measured acoustic pressure oscillations. The objective of the analysis was to determine the dependence of the flame and flow characteristics upon the flow Mach number, temperature, oxygen content and fuel to air momentum ratio. The investigated flame and flow characteristics included distribution of heat release within the combustion region and the frequencies and amplitudes of excited asymmetrically shed vortices, first explained by Bérnard/von-Kármán. Tests were performed over a wide range of incoming Mach numbers, fuel-air ratios and V-gutter flame holder widths. It is shown that the intensity of von-Kármán oscillations increases as both equivalence ratio and the momentum ratio increase.

CHAPTER 1

INTRODUCTION

Bluff bodies are commonly used to stabilize a flame in high-speed flows in propulsion and industrial systems such as industrial energy production, ramjets, and turbojet afterburners[1]. To hold a flame in a high speed flow requires an area where the velocity is not greater than the flame speed and flame blow-off occurs when the time for the reactants to ignite exceeds the time available in the combustor for the chemical reaction[2]. This low velocity zone can be accomplished by utilizing a bluff body in the flow to create a recirculation zone of lower velocity. Some factors that can influence the reaction time in the combustor are bluff-body geometry, blockage ratio, pressure, temperature, velocity, and equivalence ratio[2]. Such systems have been extensively researched over the past 60 years, with earlier studies focusing on the time-averaged characteristics of the combustion process and the development of correlations for flammability limits based on empiricism[3,4,5,6,7]. Because these flames involve complex interactions of fluid mechanics, acoustics, and combustion process heat release, steady-state characteristics do not fully describe flame blow off or the physical processes responsible for instabilities[6,7].

Flame stabilization is achieved by unburned reactants being ignited in the shear layers downstream of the bluff body trailing edge by hot combustion products recirculating behind the bluff body[4]. A portion of the newly ignited products joins the recirculation zone while some products flow downstream, continuing to burn. The continuation of this

process provides an anchor for the flame at the location where the flame encounters the bluff body[2].

Figure 1 shows a schematic of the typical structure of isothermal fluid flow around a bluff body[1]. This figure illustrates four key regions of the flow field: boundary layer formation along the bluff body, the separated shear layer, the recirculation zone just downstream of the trailing edge, and the wake. The separated shear layers consist of coherent vortices of opposite sign that roll up and are shed symmetrically downstream of the bluff body, as shown in Figure 1. For Reynolds numbers beyond a critical value (approximately 50 for a cylinder), the wake of the isothermal flow is dominated by alternating shedding of large, coherent vortices of opposite sign, leading to the sinusoidal flow field depicted in the figure. This asymmetric vortex shedding is due to the Bénard / von-Kármán (BVK) instability and is an absolute, or self-excited, flow instability[1], whereas the shear layer rollup is controlled by the convective Kelvin-Helmholtz instability.

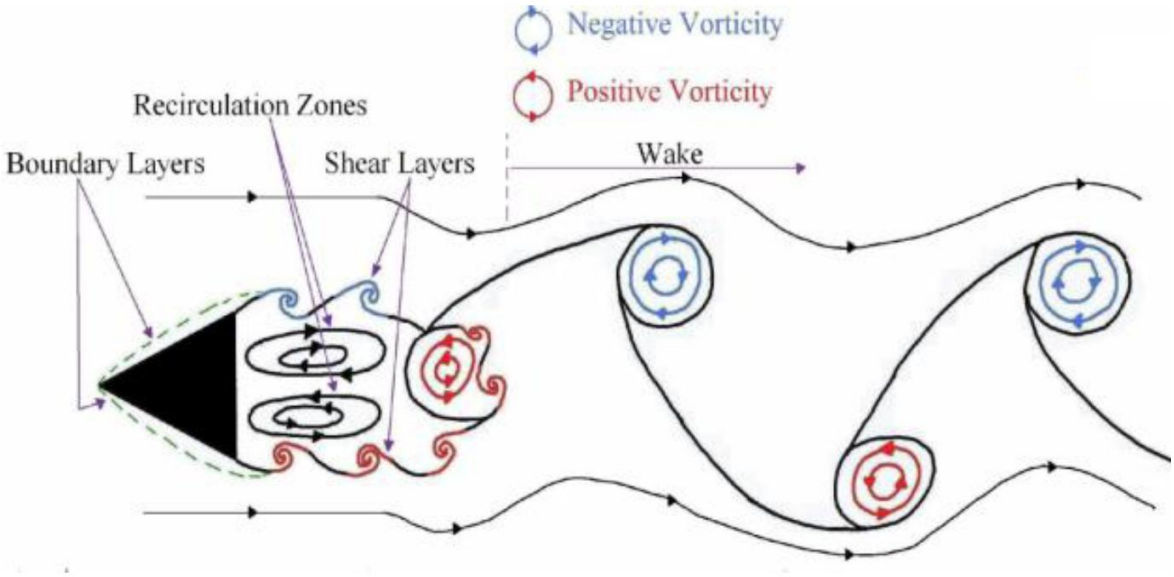

Figure 1. Fluid Mechanics of Isothermal Bluff Body Flow[1]

(Ref: Shanbhogue *et.al.* Progress in Energy and Combustion Science, Volume 5)

When combustion is present in the flow field, the exothermic heat release can significantly alter the flow structure downstream of the bluff body. Previous studies with premixed incoming reactants at low temperatures relative to the flame show that the BVK vortex street is suppressed in reacting flows, and the flame is stabilized in two distinct shear layers[1,3,4,6,8,9,10,11,12]. This is believed to be primarily caused by gas expansion due to the large dilatation ratios (ρ_u/ρ_b) resulting from the relatively high temperature ratio of the burned products to the unburned reactants (or T_b/T_u). The density jump across the flame also creates a misalignment of pressure and density gradients, and counter-acting vorticity is generated by the baroclinic mechanism. However, some studies have shown BVK flame oscillations to appear near blow out conditions even if the incoming reactant temperature is low relative to the flame temperature[1,9,10,11,13,14,15]. This is most likely due to the reduced dilatation ratio resulting from the lower flame temperature that occurs at

the very lean or rich conditions near the blowout limit. Previous studies suggest that asymmetric vortex shedding could play a key role in the loss of static stability of the bluff body flame operating near blow off[7,8].

When the incoming reactant temperature is high (as is the case for gas turbine combustors and ramburners) the temperature rise across the flame is reduced, and the flow field begins to revert to that of the non-reacting case shown in Figure 1. As a result, asymmetric vortex shedding is expected to be more dominant at the lower dilatation ratios that result from higher inlet temperatures. This was demonstrated in a numerical study by Erickson et.al., who performed a parametric study on the effect of temperature ratio on the vorticity dynamics[8]. The authors were able to show a complete transition in the distribution of the reaction zone from asymmetric vortex shedding at temperature ratios less than 1.5, to flame stabilization in two distinct shear layers at $T_b/T_u \sim 2$. The authors note, however, that these temperature ratio values are specific to the geometry and flow conditions they modeled and are by no means a universal result. It should also be noted that demonstration of the transition between symmetric and asymmetric modes of vortex shedding in a laboratory combustor is limited at best to this date, with the exception of the previously-mentioned transitions near blow out.

In bluff-body stabilized flames, flame oscillations are due to both the fluid mechanic instabilities (such as vortex shedding) and transverse and longitudinal acoustic oscillations, which can lead to system failures. Previous studies, using premixed fuel mixtures, found that asymmetric vortex shedding, or the Bénard-von-Kármán instability, is a precursor and contributor of flame blow off[9]. High-dilation-ratio flames are stabilized in two distinct shear layers and remain fluid dynamically stable, but when the

dilation ratio is decreased, the shear layers can interact and asymmetric vortex shedding can occur, which can lead to the loss of static stability in the flame[1,8,11,10,13,14,15]. Fluid mechanic instabilities may even excite natural acoustic and bulk-mode oscillations in the combustor, especially when the resonant frequency of the combustor is near the frequency of the vortex-shedding first mode or a harmonic.

Past research focused mainly on the static and dynamic stability of premixed combustion. These studies have found that both fluid mechanic and kinetic processes contribute to blow off such that near blow off, shear layers dominated by the Kelvin-Helmholtz instability occur immediately downstream of bluff body trailing edge, while further downstream, the wake is characterized by von-Kármán vortex shedding [9,16]. This has been validated theoretically, experimentally, and with Large Eddy Simulation. However, real life implementation of bluff body flows does not usually allow for the use of premixed fuels, requiring injection of the fuel as liquid jets into the flow. This method of fuel injection adds more parameters to our system, such as mixing time and auto ignition time of the fuel spray and results in a non-uniform distribution of fuel throughout the flame, giving areas of locally lean and rich fuel distribution[17]. Since the combustion process greatly affects the stability of the flame, experimental results on this topic would be beneficial.

The goal of this research was to investigate the combustion dynamics of non-premixed, V-gutter-stabilized flames while fuel is injected in cross-flow fuel injection just upstream of the V-gutter. Flame blow off refers to the situation in which the flame is no longer stabilized and is detectable and preventable by determining the symptoms of flame blowout through observing the dynamics of unstable flames. This study seeks to

determine how the flame is stabilized during operation when the dilation ratio is relatively high and how this pattern changes as the lean and rich flammability limits are approached, specifically, how changes in heat release distribution leads to changes in the intensity of von-Kármán vortex shedding. This was done by using optical diagnostics such as high speed movies and time-averaged chemiluminescence images of the flame at multiple flow conditions, with varying inlet Mach numbers, fuel-air ratios, and V-gutter widths. The high speed movies were processed using a new technique to determine the dominating frequencies in the flame, focusing on the longitudinal-acoustic oscillations and von-Kármán asymmetric vortex shedding. Using this data, the frequencies and amplitudes of oscillation of the flame for the longitudinal and von-Kármán modes can be measured along the length of the combustor. The time-averaged chemiluminescence images show the distribution of heat release throughout the flame and can be integrated to find the total heat release. Using both the amplitudes of flame oscillations found using the high speed camera and the distributions of heat release from the time–averaged images, the effect changes in the distribution of high heat release has on the combustion instabilities can be determined.

Theory predicts that higher heat release in the shear layers of the flame, will lead to lower amplitudes of von-Kármán vortex shedding. This theory was investigated. A method was developed to quantify the heat release in the shear layers of the flame using the CH* heat release images and these intensities were compared with oscillatory heat release data to determine the relationship between the intensity of shear layer heat release and flame oscillation. Because fuel placement affects the locations of high intensity heat release, the

effect of the fuel jet momentum flux on the intensity of von-Kármán asymmetric vortex shedding was investigated.

The study was carried out in Georgia Tech's single flame holder combustor test facility with a high-temperature inlet air supply. The facility's transparent test section allowed for full optical access to the flame and fuel spray and allowed tests to be run with high-temperature, low oxygen incoming through use of a pre-burner. This study focused on the oscillatory heat release measurements found by recording and post-processing of high speed movies and introduced a methodology developed to quantify the frequencies and intensities of flame oscillation due to acoustically-coupled and hydrodynamic instabilities[18].

CHAPTER 2

EXPERIMENTAL METHODOLOGY

Description of Test Facility and Instrumentation

Experiments were performed in the single flame holder combustor (SFC) test facility at Georgia Tech's Ben T. Zinn Combustion Laboratory, shown in Figure 2 and Figure 3. This facility consists of a pre-burner, flow-conditioning section, and test section.

Figure 2. Photograph of SFC Test Facility

The test section is 3"x6"x60" and includes a 36" quartz window allowing for optical access to the combustion region. V-gutter flame holders are attached to an aerodynamically shaped support plate and incorporate four plain cross-flow injectors. The quartz windows are air cooled to prevent thermal expansion and window cracking. Operation at elevated inlet temperatures is achieved by burning natural gas with preheated air, producing a vitiated air supply to the test section. Diluting air allows for control of the air flow rate, temperature, and oxygen content of the combustor. Incoming air temperature, pressure and oxygen content are measured immediately upstream of the test section using thermocouples, a Pitot tube, and an O_2 sensor, respectively. This rig uses a 100 Hz data acquisition system to record 64 channels of pressure, temperature,

flow rates, etc. and a Sony 16 channel data recorder operating at up to 48,000Hz for recording pressure oscillations by Kistler type sensors installed in semi-infinitive tubes.

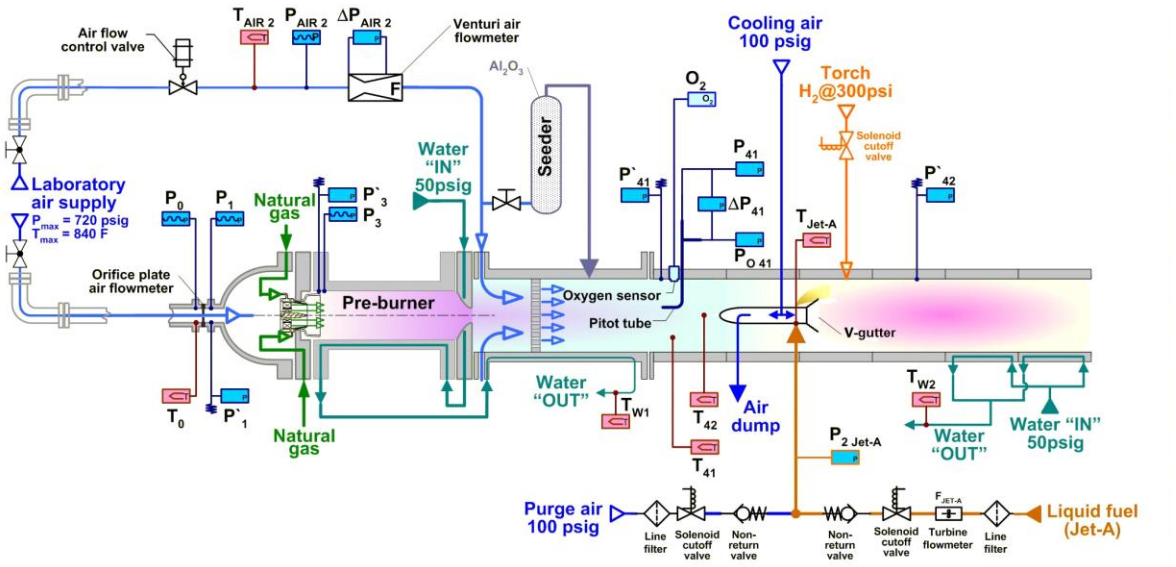

Figure 3. Schematic of Single Flameholder Combustor (SFC) Test Facility identifying major components of the rig and V-gutter flame holder

Using High Speed Photography to Quantify Oscillatory Heat Release

Using a NAC GX-1 high-speed camera at 10,000 Hz, high speed movies were recorded at a resolution of 908x176 pixels with an exposure time of 12 μs in only blue and green channels, which contain the CH* and C_2* chemiluminescence. A method was developed at Georgia Tech that quantitatively evaluates the flame dynamics by converting spatial frames from high speed movies to temporal ones, resulting in a time series image of flame oscillations at a particular cross-section.

A time history of the flame at each cross-section in the combustor was created using the methodology illustrated in Figure 4. Methodology for recording flame dynamics at a

given cross section For each frame in the movie sequence (marked N), a thin strip (1 pixel wide) of the flame image at the given axial location was extracted. These strips were then "stacked" in chronological order to produce the time dependence of the light intensity at the given cross-section, as shown in the figure.

In the time history, each row represents a time history of a single pixel in the movie.

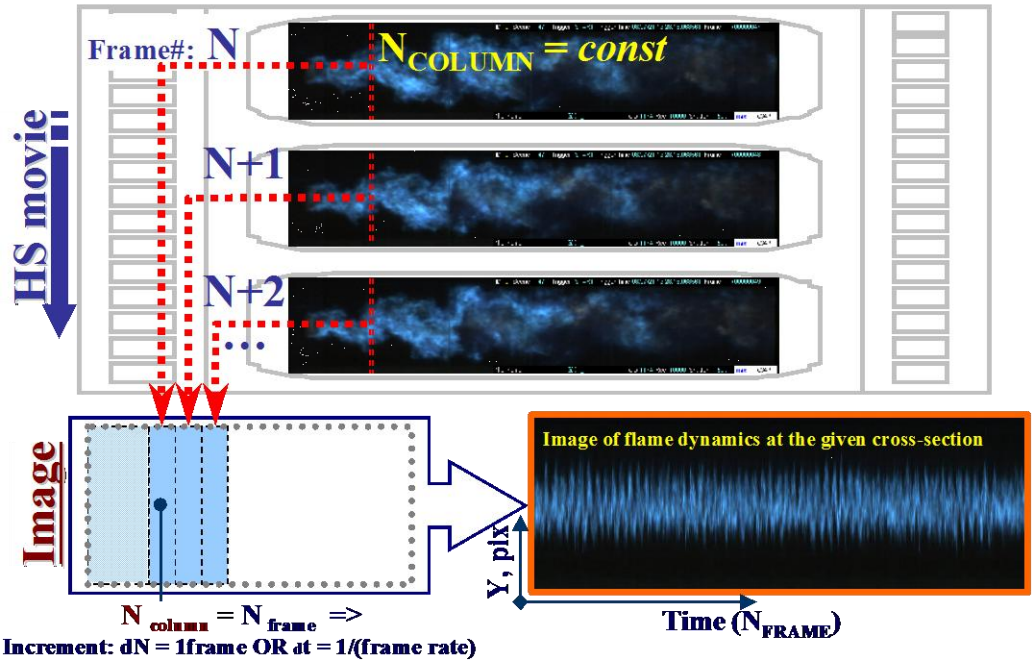

Figure 4. Methodology for recording flame dynamics at a given cross section

A two dimensional Discrete Fourier Transform, which changes the domain from time to frequency, was performed on the time series to determine the amplitudes and frequencies of the dominant oscillatory modes. This results in a new 2D image in which the horizontal axis represents the frequency of flame oscillations (Hz) and the vertical axis represents a spatial frequency with units of 1/length. An example of the 2D DFT output when applied to our study is shown in Figure 4. The amplitude at a particular frequency is represented by the pixel intensity in the Fourier image. By extracting horizontal cross

sections of the intensity vs. frequency plane at different vertical coordinates, conventional, one-dimensional power spectra can be produced, as shown in Figure 5c-d.

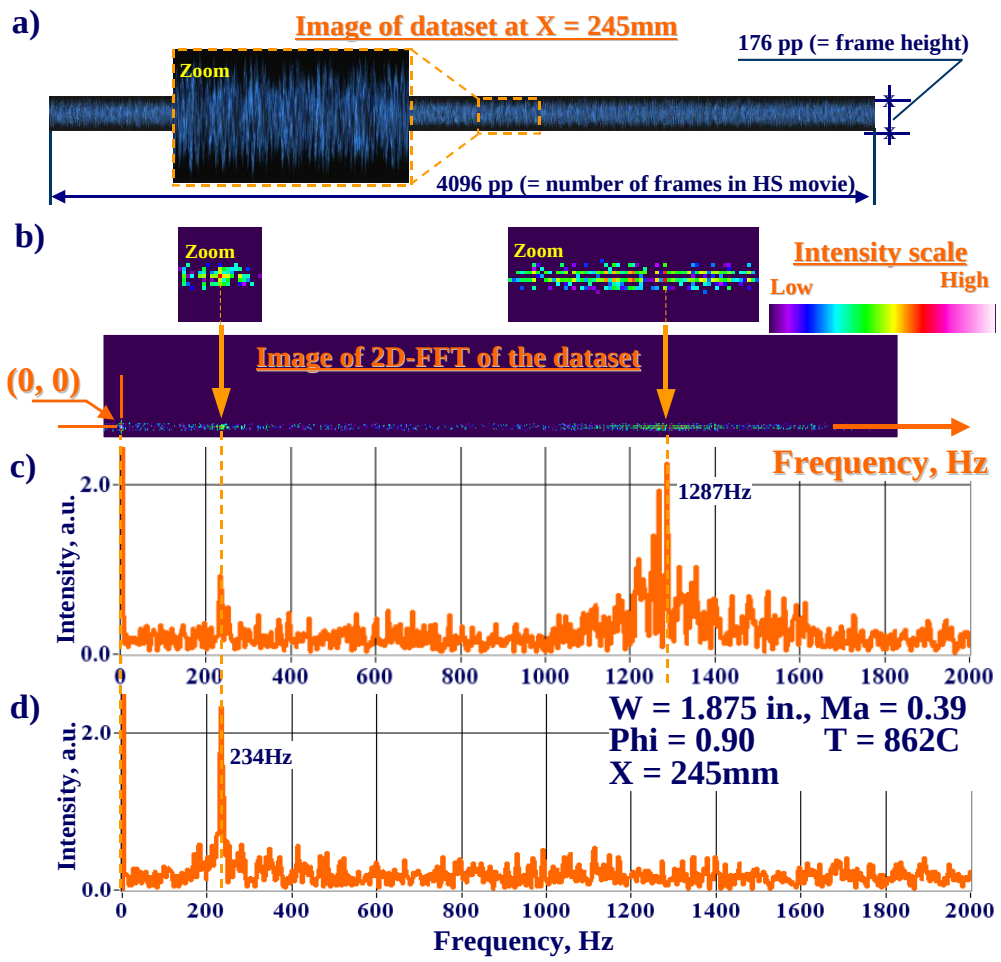

Figure 5. 2D Digital Fourier Transform (DFT) of the time history data set and method for generating spectra of flame oscillations, showing:

a) Image of the time history data set recorded in the cross-section of the combustor 245 mm downstream of the flame holder trailing edge.

b) Image of the 2D DFT of the data set presented in Fig 8-a (above)

c) Spectrum, characterizing mainly von-Kármán (*f* ~1280 Hz) instability

d) Spectrum, characterizing longitudinal (*f*=234 Hz) instability

Quantification of Stationary Heat Release Using 3-Camera Spectrometry System

Spatial distributions of the time-averaged heat release were measured by the use of a newly developed flame spectrometry system. This technique makes use of three high-definition cameras, each with a 2 megapixel spatial resolution (~ half of which focused on the flame pattern), which take wavelength-specific images of the flame. Figure 6 shows a schematic of the camera and filter setup used to collect this data.

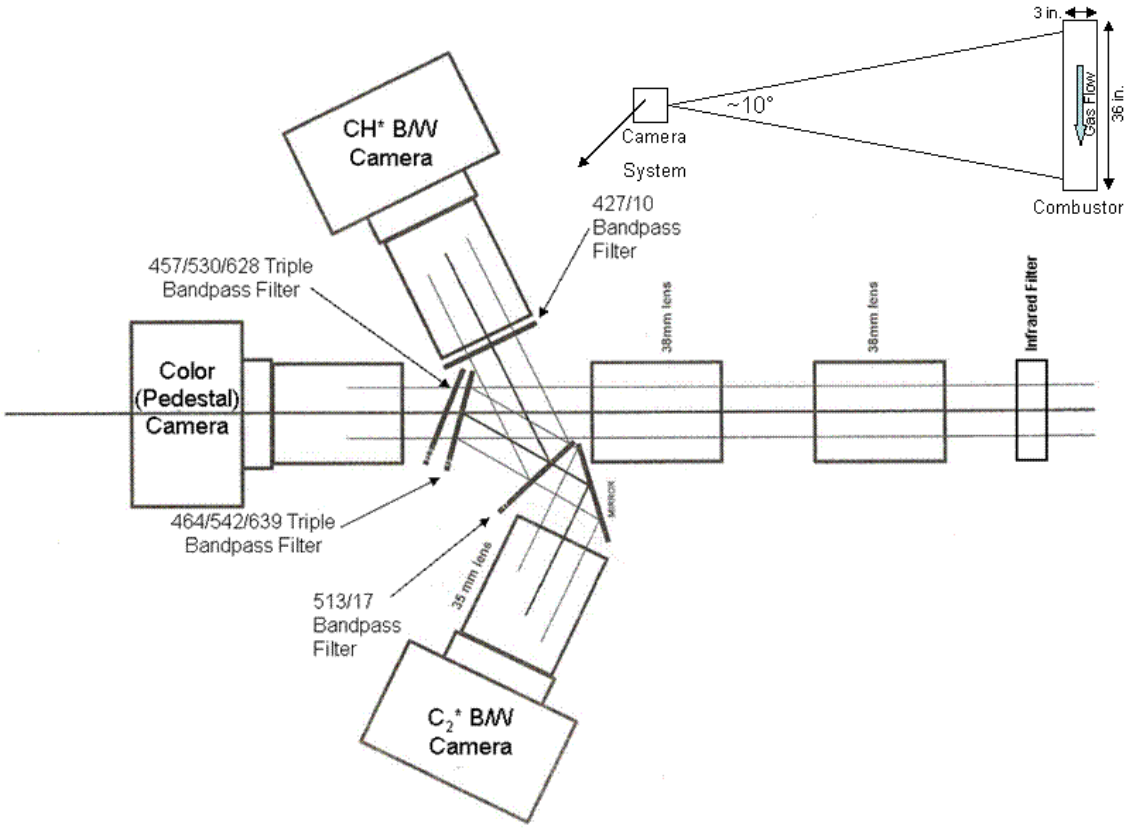

Figure 6. Schematic of three-camera technique used for mean heat release characterization

Two of the cameras (black and white) are equipped with narrow band-pass filters to collect light intensity in bands typical of C_2* ($504 < \lambda < 521$) and CH* ($422 < \lambda < 432$) light emission. The third camera is a color camera equipped with two triple-band pass filters (see Figure 6 for wavelengths) to collect flame radiation in three specific narrow bands for subtraction of background radiation (due to CO_2*, water, soot, etc.) in the CH* and C2* images, as shown in Figure 7. The resulting CH* and C2* images (with subtracted background) were then used to characterize the stationary heat release. The post-processing algorithm was adjusted by comparison of stationary heat release data obtained using this 3-HD camera measurement technique to that recorded by scanning the flame with a spectrometer at the same flow conditions. This allowed for determining the proper "pedestal" bands of light for background subtraction, which are shown in Figure 7.

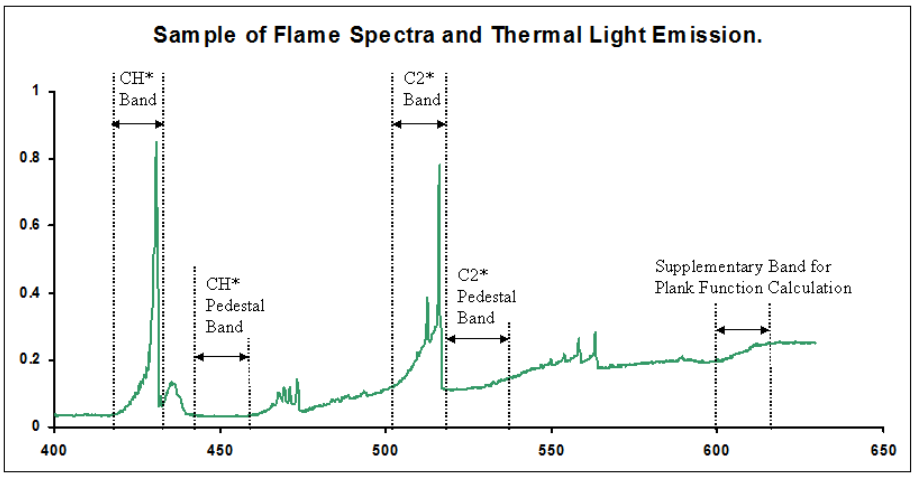

Figure 7. Measured Jet-A flame spectra and light bands used for image processing

CHAPTER 3

RESULTS AND DISCUSSION

The dynamic and stationary heat release was characterized over a wide range of inlet velocities, temperatures, and overall fuel-air ratios and v-gutter widths using the diagnostic techniques described in the previous chapter. Four v-gutter widths (2.250", 2.000", 1.875" and 1.750") were tested at various inlet velocities, and overall fuel-air ratios. At each flow condition average CH* and C2* spectrometry images and high speed movies were recorded. All together, approximately 70 combinations of incoming flow parameters were tested. Due to the varying test conditions it was useful to use DeZubay's empirical correlation to relate these tests. DeZubay's correlation, defined below, considers velocity, temperature, v-gutter width and pressure, and represents a stability parameter for bluff-body-stabilized flames. Although, it was developed for pre-mixed flames and does not consider close-coupled injection influences such as fuel-air momentum ratio.

$$DeZubay'sParameter \equiv \frac{V}{P^{0.95}D^{0.85}}\left(\frac{T}{T_0}\right)^{1.5}$$

A summary of these test conditions is shown in Figure 8 as a plot of global equivalence ration versus DeZubay's correlation. In Figure 8, the rich flammability limit is shown by an estimated line based on the observation of operating conditions near rich blowout.

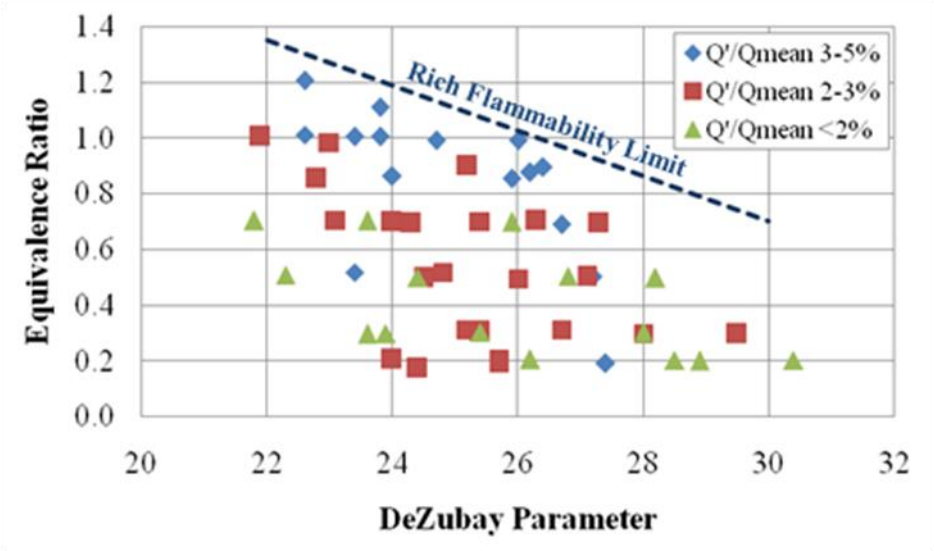

Figure 8. Summary of experimental operating conditions expressed as Φ_{global} vs. DeZubay's Correlation

Oscillatory Heat Release

Measurements of Flame Oscillations due to BVK Asymmetric Vorticity

A sequence of five images showing one period (~0.8ms) of BVK flame oscillations is shown in Figure 9. These images were extracted from the high-speed movie of a flame at flow conditions that resulted in large BVK oscillations (f~1210Hz at Vin=230m/s, Φ_{global}~0.95, T=860ºC). The time increment between frames is 0.2ms, with "time stamps" labeled on each image. The vertical dashed line crossing these images and coinciding with the first "crest" of these sinusoidal flame movements on the first and last frames (marked τ=0 ms and τ=0.8 ms, respectively) clearly indicates convection of this structure along the combustor.

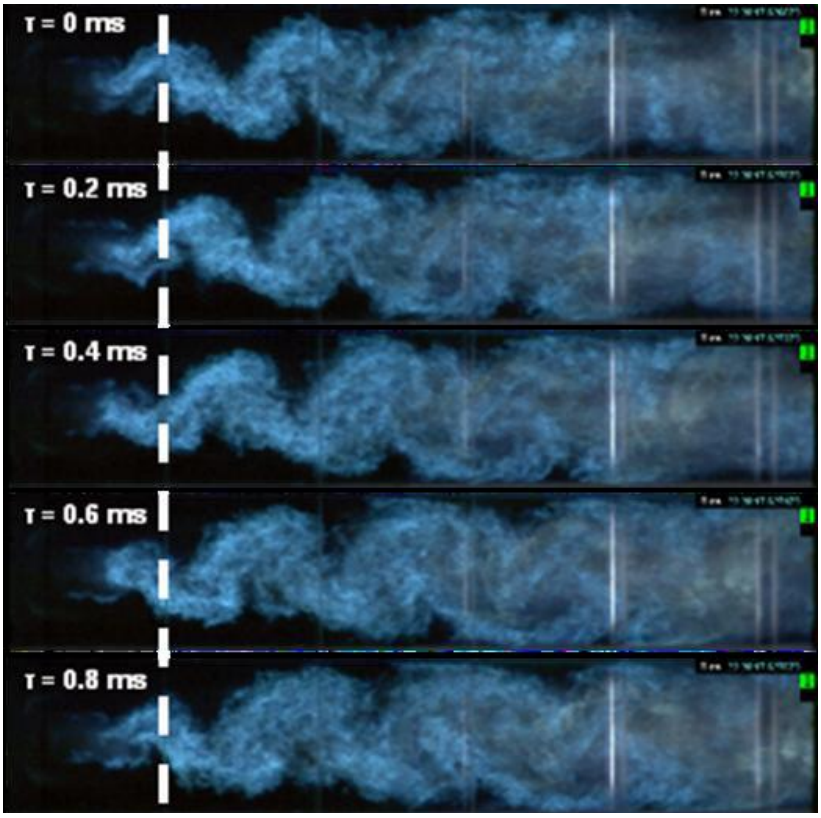

Figure 9. Sequence of flame images representing one period of BVK Oscillations. Flow conditions: V_{in}=230 m/s, T=860ºC, Φ_{global}~0.95

The technique outlined in Figure 5 was used to determine the peak amplitude of BVK oscillations at each axial location along the combustor. Shown in Figure 10 is (a) the resulting time history, (b) 2D DFT, and (c) spectra of a flame oscillating due to BVK vortex shedding (at flow conditions: M=0.340, Φ =0.991, 859°C, 14.43% O_2, W=1.750in) calculated at a cross section approximately 6 inches downstream of the bluff body. The 2D DFT shows bright area near the frequency of BVK oscillations for these conditions and the cross-sectional spectrum shows a peak intensity at 1091Hz.

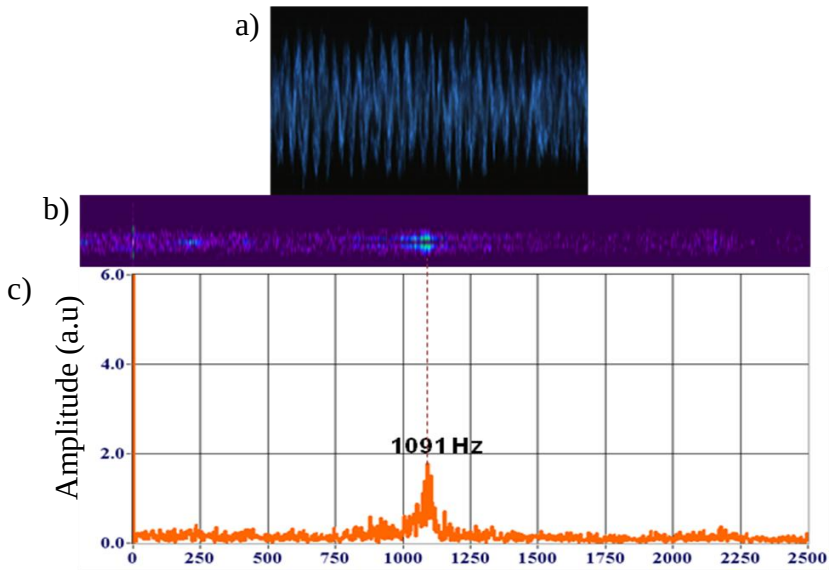

Figure 10. (a) Time history, (b) 2D DFT, and (c) spectra of flame at M=0.340, Φ =0.991, 859°C, 14.43% O2, W=1.750in

This procedure was repeated at every axial location along the combustor (every column of pixels in the images) and results in a plot showing the variation of BVK oscillations along the combustor. Figure 11 shows this variation for the same test as shown in Figure 10 (M=0.340, Φ =0.991, 859°C, 14.43% O_2, W=1.750in). The axial distributions of the amplitudes are very similar for each operating condition, showing a peak at approximately 4-5 bluff-body widths downstream of the trailing edge before gradually decreasing. The maxima of the flame oscillation amplitudes from these axial plots were used as a measure of the overall intensity of the BVK mode of flame oscillations.

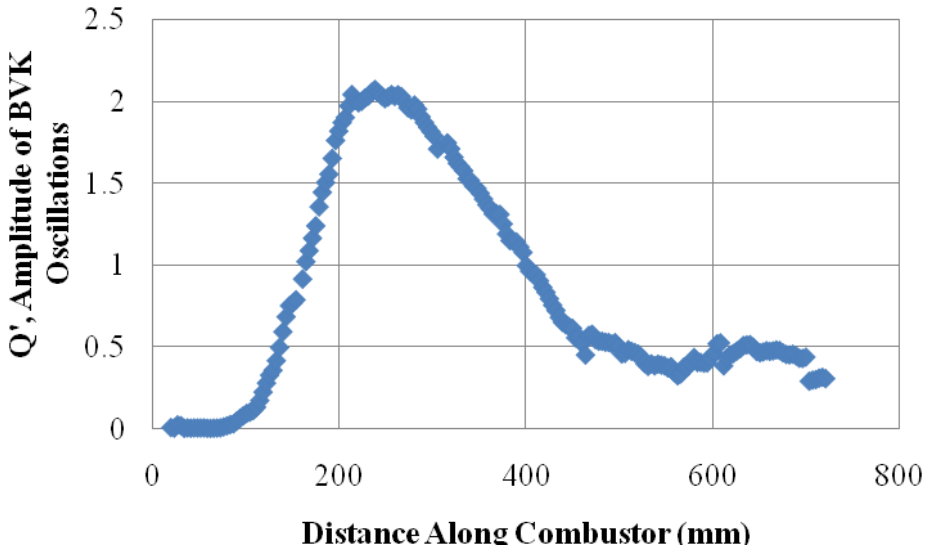

Figure 11. Variation of Q' along the axial length of the combustor.

Von-Kármán Asymmetric Vortex Shedding

Using the maxima of BVK flame oscillations, a plot was made showing the dependence of these oscillations on incoming fuel-air equivalence ratio, or Φ_{global}. This plot is shown in Figure 12. For all incoming Mach numbers, the intensity of oscillations remains relatively constant as equivalence ratio is increased until reaching approximately Φ=0.7. At this point the intensity of oscillations increases with further increase in equivalence ratio.

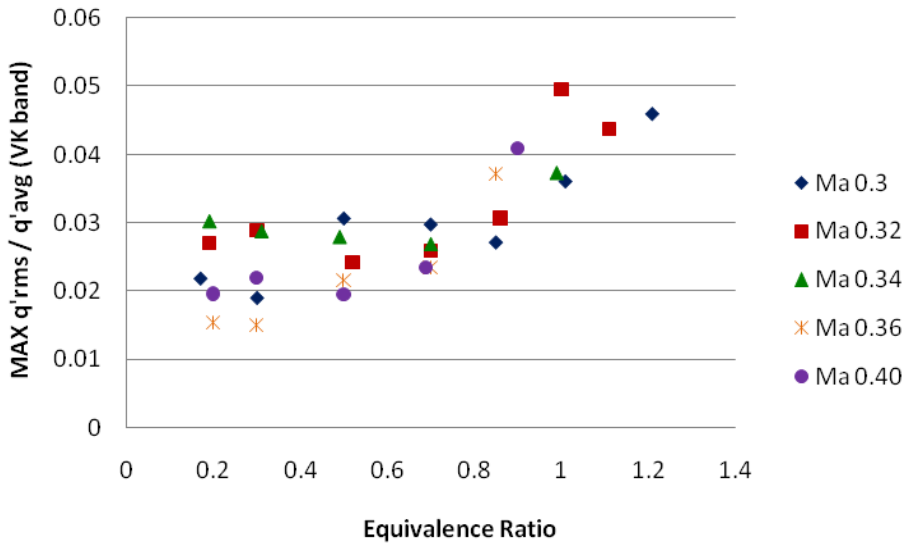

Figure 12. Dependence of Von-Kármán oscillation intensity on equivalence ratio

The behavior of Figure 12 may be explained by the interaction of close-coupled fuel injection. Therefore, the fuel-air momentum flux ratio was calculated for all test conditions using a measured fuel flow rate and measured upstream Mach number. Isentropic relationships were used to find lip Mach number based on the area change in the combustor. Using high speed imaging of a fuel spray, a relationship was developed to calculate fuel penetration at various distances from the injectors using fuel-air momentum flux ratio and constants and it was found that fuel penetration is proportional to the product of the square root of fuel-air momentum flux ratio (q) and natural log of the ratio of the distance from the fuel injector in inches (z) to the fuel injector diameter (d) as shown below:

$$\frac{x}{d} \sim \sqrt{q} \ln\left(\frac{z}{d}\right)$$

The penetration was found at a distance of 1 inch from the fuel injectors, which corresponds to the approximate end of the flame holder. Using these calculated values for penetration, plots were made showing the relationship between von-Kármán intensity and the ratio of penetration to V-gutter width. First, the intensity was compared to the standard V-gutter width, measured from edge to edge. Then the V-gutter displacement was used, measured from the bluff body support plate to the edge of the V-gutter. These plots and schematics of measurements are shown in Figure 13. These plots show a similar relationship as von-Kármán intensity with equivalence ratio. They are fairly constant until 0.02 for penetration divided by width and 1.0 for penetration divided by V-gutter displacement. Note that for a ratio of penetration to V-gutter displacement of less than one the fuel is deflected from the V-gutter to the shear layer instead of being deposited directly into the flame.

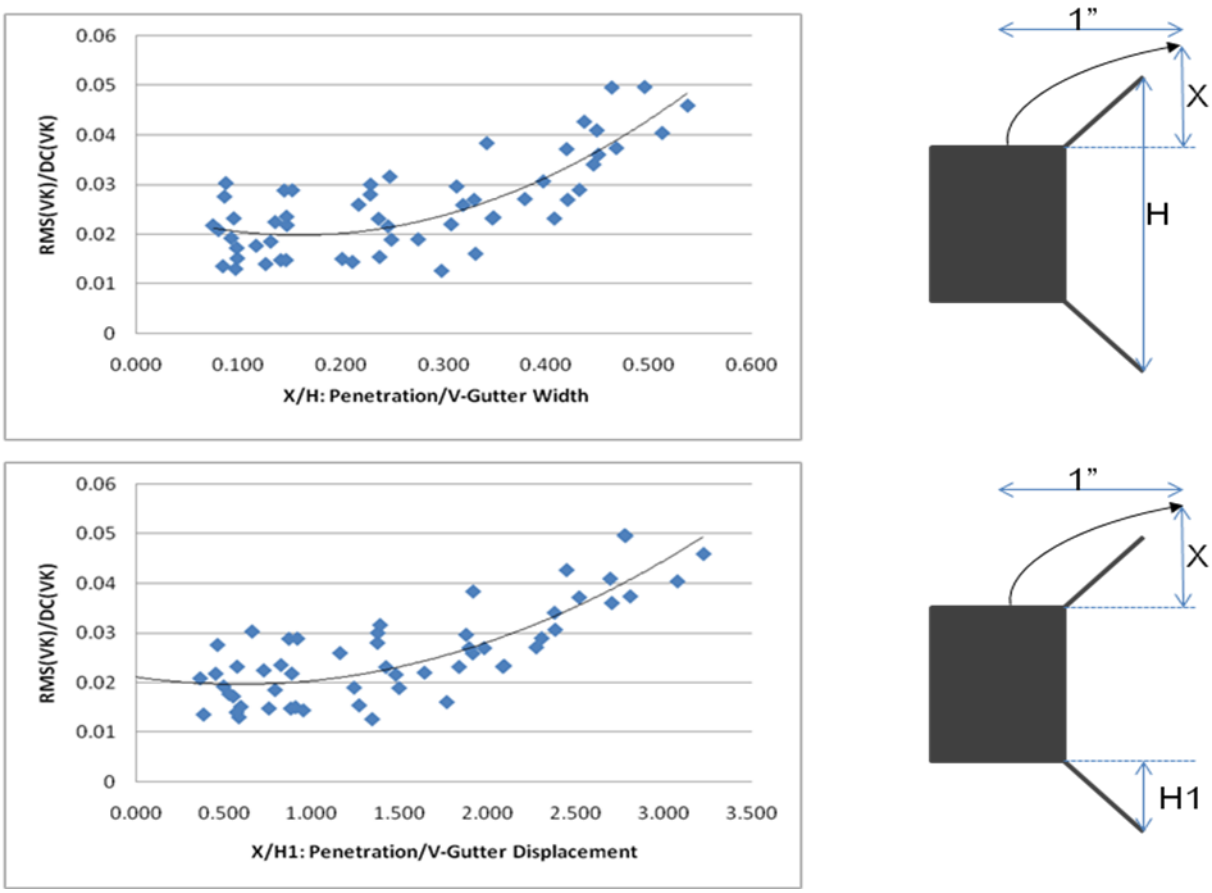

Figure 13. Intensity of von-Kármán oscillations versus fuel-jet penetration

Stationary Heat Release

The previously described 3-camera flame spectrometry methodology can be used to characterize the distribution of heat release throughout the flame and may explain the dynamic heat release behaviors observed. A series of time-averaged CH* chemiluminescence images are shown in Figure 14 for flow conditions of Ma=0.39, T=838°C, and W=2.00in. At a low equivalence ratio, Φ=0.200-0.504, the flame is stabilized in two bright, symmetric shear layers with the intensity and size of these shear layers changing slightly with equivalence ratio. As the equivalence ratio is increased, the

flame becomes longer and the shear layer heat release becomes less intense. For Φ=0.698 these areas of intense reaction convect further downstream than the near-field shear layers, and for Φ=0. 90 these bright areas have moved even further downstream and are merging into the wake of the bluff body. Note that in the first 2-3 v-gutter widths there is very little reduction in heat release intensity in the shear layers.

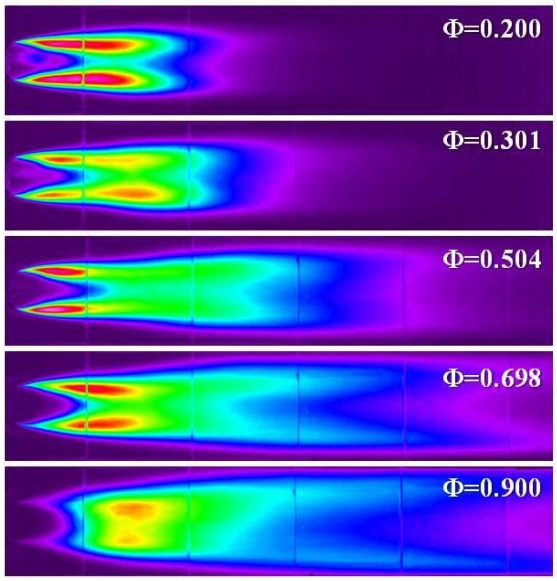

Figure 14. Stationary Heat Release Images for M=0.390, T838°C, W=2.000"

Using these stationary heat release images, the intensity of CH* was averaged along every vertical cross-section. This was plotted along the length of the combustor and to eliminate a changing variable, all average CH* profiles were normalized by fuel flow rate and show intensity of heat release per unit of fuel consumption in g/s. An example of these profiles is shown in Figure 15 and shows the CH* distribution for various test conditions with constant DeZubay parameter. Referring to the stability map shown in Figure 10, these conditions fall along the vertical line at Z=24 and range from low

equivalence ratio to the rich blow out limit. The greatest difference in profiles occurs from 5 to 15 inches along the combustor, which is slightly downstream of the fuel entrainment zone.

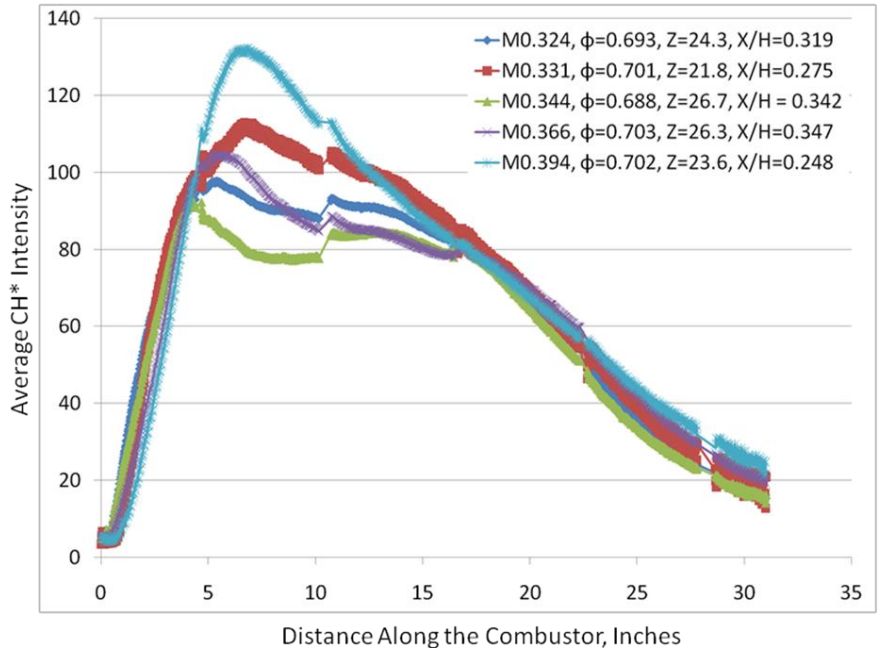

Figure 15. Average CH* Profile for Constant DeZubay Parameter

To determine the effect of changes in heat release distribution on the intensity of BVK oscillations, and to investigate the hypothesis that these oscillations are dependent on the fuel stabilization in the shear layers, heat release was summed inside of an area designated as the shear layer and compared to the intensity of oscillations. This area was defined as a 100x300 pixel wide box centered on the top or bottom edge of the flame holder, as shown in Figure 16.

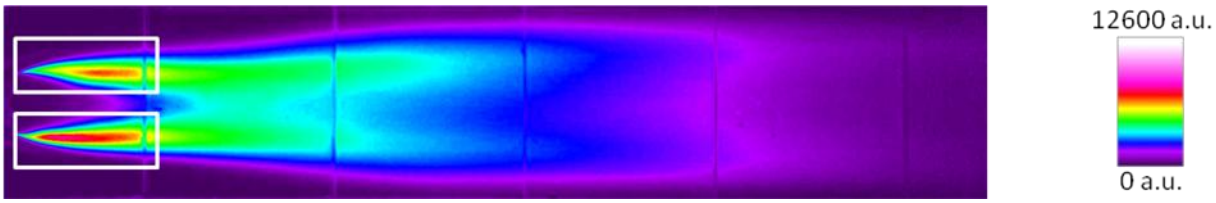

Figure 16. Shear layer definition (M=0.348, T=764C, Phiglobal=0.512)

The total heat release intensity in the shear layers was calculated for each test condition and normalized by the total heat release of each image. The plot of BVK intensity versus this ratio of heat release is shown in Figure 17. Above 3% heat release in the shear layers, increasing this ratio results in relatively constant BVK oscillations of 2% of the average heat release component. Below 3% heat release in the shear layers, a decrease in this ratio causes an increase in the intensity of BVK oscillation to a maximum for 5% for these tests.

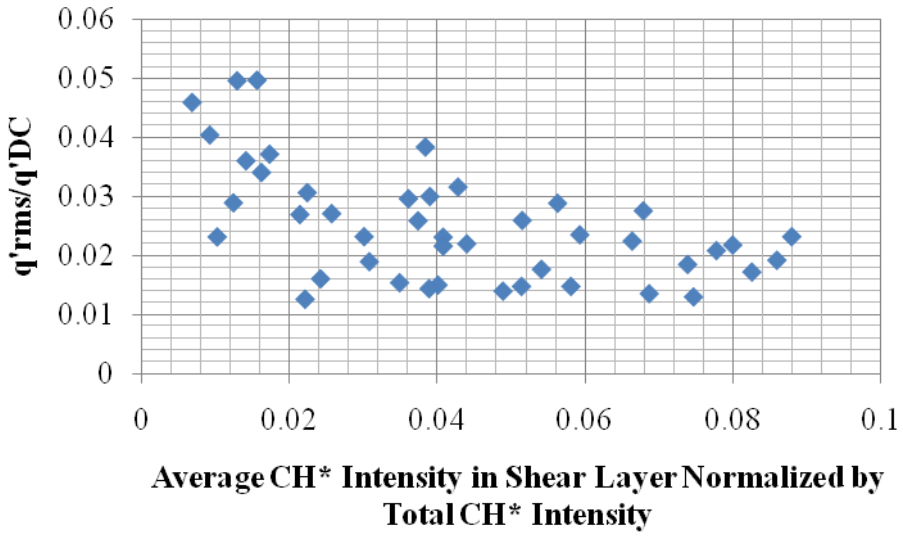

Figure 17. BVK Oscillation Intensity versus the ratio of heat release in the shear layer

CHAPTER 5

CONCLUSIONS

- The methodology developed at Georgia Tech to quantify the dominating frequencies and amplitudes of oscillation of a flame, using dynamic heat release, is capable of revealing the BVK oscillatory modes in this combustor. This methodology involves creating a time history of flame dynamics from a high speed movie and using this time history to create a 2D DFT and conventional, one-dimensional, flame spectra.

- It was shown that the intensity of von-Karman asymmetric vortex shedding increases with equivalence ratio and fuel penetration and high intensity oscillations occur nearer to the point of flame blow-off as determined experimentally and shown in the stability map.

- For this combustor, BVK oscillations remained relatively constant as equivalence ratio increased until reaching a limit at Φ=0.7, after which increases in equivalence ratio led to an increase in flame oscillations.

- The three camera spectroscopy methodology is capable of capturing the CH* and C2* intensity over the entire flame. By applying a color filter to these resulting images, the patterns of heat release distribution are easily visible. The images can be integrated to show the heat release along the combustor and reveal similar profiles with most difference occurring 5 to 15 inches from the bluff body.

- A comparison of the dynamic and stationary heat release shows a dependence of BVK flame oscillations on the ratio of the heat release in the shear layer, as defined by a 100x300 pixel wide box, to the total heat release in the time-averaged image. Above 3% heat release in the shear layer, increases in this ratio do not cause changes in flame oscillations, while below 3% a decrease in the heat release in the shear layer causes an increase in flame oscillations.

REFERENCES

[1] Shanbhogue, S., Husain, S., and Lieuwen, T., "Lean blowoff of bluff body-stabilized flames: Scaling and dynamics," *Progress in Energy and Combustion Science*, 35, pp. 98-120, 2009.

[2] Lefebvre, Arthur. Gas Turbine Combustion. Second Edition. Edwards Brothers, Ann Arbor, Michigan, 1999.

[3] Zukoski, E.E., "Afterburners," *The Aerothermodynamics of Aircraft Gas Turbine Engines*, AFAPL-TR-78-52, G. Oates, Editor, 1978.

[4] Zukoski, E. E., and Marble, F. E., "Experiments Concerning the Mechanism of Flame Blowoff from Bluff Bodies," *Proceedings of the Gas Dynamics Symposium on Thermochemistry*, Northwestern University, Evanston IL, 1956, pp. 205-210.

[5] Longwell, J.P., Chenevey, J., Clark, W. and Frost, E., "Flame Stabilization by Baffles in a High Velocity Gas Stream," *Proceedings of the Combustion Institute*, Vol. 3, 1951, pp. 40-44.

[6] DeZubay, E. A., "Characteristics of Disk-Controlled Flames," *Aero Digest*, Vol. 61, No. 1, July 1950, pp. 54-56.

[7] Ozawa, R.I., "Survey of Basic Data on Flame Stabilization and Propagation for High Speed Combustion Systems," AFAPL-TR-70-81.

[8] Erickson, R.R., Soteriou, M.C. and Mehta, P.G., "The Influence of Temperature Ratio on the Dynamics of Bluff Body Stabilized Flames," *44th Aerospace Sciences Meeting and Exhibit*, Reno, Nevada, AIAA Paper #2006-753.

[9] Lieuwen, T., Shanbhogue, S., Khosla, S. and Smith, C., "Dynamics of Bluff Body Flames near Blowoff," *45th AIAA Aerospace Sciences Meeting and Exhibit*, 2007, Reno, Nevada, AIAA Paper No. 2007-0169.

[10] Kiel, B., Garwick, K., Lynch, A., Gord, J. R. and Meyer, T., "Non-Reacting and Combusting Flow Investigation of Bluff Bodies in Cross Flow", *42nd AIAA/ASME/SAE/ASEE Joint Propulsion Conference and Exhibit*, Sacramento, California, AIAA Paper #2006-5234

[11] Hertzberg, J. R., Shepherd, I. G., and Talbot, L., "Vortex Shedding Behind Rod Stabilized Flames," *Combustion and Flame,* Vol. 86, 1991, pp. 1-11.

[12] Mehta, P.G., and Soteriou, M.C., "Combustion heat release effects on the dynamics of bluff body stabilized premixed reacting flows,' AIAA Paper # 2003-0835.

[13] Fureby, C., "A Computational Study of Combustion Instabilities due to Vortex Shedding," *Proceedings of the Combustion Institute*, 28, pp. 783-791, 2000.

[14] Thurston, D.W., "An Experimental Investigation of Flame Spreading from Bluff Body Flameholders," PhD Thesis, California Institute of Technology, Pasadena, CA (1958)

[15] Smith, C., Nickolaus, D., Leach, T., Kiel, B. and Garwick, K., "LES Blowout Analysis of Premixed Flow Past V-Gutter Flameholder", *45th AIAA Aerospace Sciences Meeting and Exhibit*, Reno, Nevada, AIAA Paper#2007-170.

[16] Smith, C., Nickolaus, D., Leach, T., Kiel, B. and Garwick, K., "LES Blowout Analysis of Premixed Flow Past V-gutter Flameholder." *45th AIAA Aerospace Sciences Meeting and Exhibit*, 2007, Reno, Nevada, AIAA Paper No. 2007-170.

[17] Lovett, J., Brogan, T., Philippona, D., Keil, B., Thompson T., "Development Needs for Advanced Afterburner Designs," *40th AIAA/ASME/SAE/ASEE Joint Propulsion Conference and Exhibit*, 2004. AIAA Paper No. 2004-4192.

[18]Shcherbik, D., Cross, C., Fricker, A., Bibik, O., Scarborough, D., Lubarsky, E., Zinn, B., "Dynamics of V-Gutter-stabilized Jet-A Flames in a Single Flame Holder Combustor with Full Optical Access," *45th AIAA/ASME/SAE/ASEE Joint Propulsion Conference & Exhibit*, 2009**,** Denver, Colorado**,** AIAA Paper No. 2009-5291.